# Aseismic Design of Machine Structure

Heki       Shibata
Hisayoshi Sato
Tatsuya    Shigeta

In §2. the evaluation method for vibration characteristics of piping systems are studied, and several examples are shown.  In §3. the machine structure is simulated into analog computer with two-degree-of-freedom system, the response spectrum analysis is performed and the general principle of aseismic design is investigated.  It is discussed that the method to obtain the maximum acceleration amplification factor for various parameter by statistical approach with the assumption, the earthquake to be a random process in §4.

## §1.  Introduction

At a nuclear power plant even a slight damage of the piping system which is related to primary coolant system in reactor core or radioactive fluid system would leads to serious hazard to human life.  To prevent such a hazardous accident under a strong earthquake condition a new design concept of piping system and machine structure should be developed. (1)

The authors have been developing them for these several years under supervising of Professor Fujii, the University of Tokyo.  A part of our jobs has been done as an activity of the Sub-committee on developing of aseismic design of machine-structure in the Japan Society of Mechanical Engineers.  At §2 the authors mainly refer to the job of Dr. Shibata and Mr. Shigeta, and §3 and §4 to the job of Dr. Sato.

The flow chart of the ascismic design is as Fig. 1.  The first step of the aseismic design is the evaluation of natural frequencies (or eigenvalues) and mode shapes of the structure.  To evaluate those of a piping system is more difficult than those of other structures.  In some cases the frequency of its fundamental mode may be extreme low and one or several higher modes may co-incide with dominant frequencies of the building and ground motion.  Moreover, by the effects of additional masses and spring occasionaly several modes may concentrate in very narrow range.

If the piping system is attached to the building-structure, lower mass system, the whole system will be able to simulate as two-degree-of-freedom system.  As for piping system each natural frequency can be dealt with as if it is one-degree-of-freedom system.  As the result of analog computation of such systems for earthquake record several principles for aseismic design of general machine structure was made clear.  And it is proposed that a simple evaluation of response acceleration using table by a statistical computation about the maximum.

## §2.  Evaluation of Natural Frequencies and Modes (2), (3)
### §2.1. Approach to coding and Computation

Institute of Industrial Science, University of Tokyo, Azabu-Shinryudocho, Tokyo

The authors use the assumption that each portion of the piping system is treated as a simple beam, that is:

(1) neglect the effect of an axial force on the flexural rigidity.
(2) neglect the effect of the shearing force and the rotating inertia.
(3) neglect the unbalance of the forces (including the gravity force) caused by the geometric deformation of the structures.
(4) neglect all sorts of internal dampings.
(5) the cross-section should be annular.
(6) neglect the distributed mass for the torsional vibration.

The transfer matrix of each straight section can be written by a matrix $[M]_i$. The transfer matrix of a whole piping system or beam is obtained by multiplying the matrices from one end to the other end.

$$[M]_{n,0} = [M]_n * [M]_{n-1} * \cdots \quad \cdots * [M]_1 \tag{2.1}$$

According to the boundary condition of both ends, some quadrant of the transfer matrix acts as the eigen value or the frequency equation of this system.

$$[M]_{n,0} = \left[ \begin{array}{c|c} M_d & M_{df} \\ \hline M_{fd} & M_f \end{array} \right]_{n,0} \tag{2.2}$$

$$\det \left| M_{df} \right| = 0 \qquad \text{for "Fix-Fix" condition} \tag{2.3}$$

We can not solve this equation explicityly, but can get the roots through the step by step change of it and iteration method. The accuracy of each root checked as the relative one between the n-1 th iteration step and the n th step.

$$\varepsilon > \left| \frac{\lambda^{(n-1)} - \lambda^{(n)}}{\lambda^{(n)}} \right| \tag{2.4}$$

The elements of the individual transfer matrix of a piece are usually some combination of trigonometric function and hypabolic one. (Table 1) Vector $Q$ represents a dimensionless displacement and force vector.

$$Q = \begin{bmatrix} \overline{y} \\ \overline{\alpha} \\ \overline{f} \\ \overline{m} \end{bmatrix} = \begin{bmatrix} y / \frac{L}{\lambda} \\ \alpha \\ f / \frac{\lambda^2 EI}{L} \\ m / \frac{\lambda EI}{L} \end{bmatrix} \tag{2.5}$$

$y$ : displacement

$\alpha$ : gradient    $L$ : length

$f$ : force    $EI$ : flexural rigidity

$m$ : moment    $\rho$ : line density

In the transfer matrix of the original form (4), derivatives or integrals of the vector elements with respect to the co-ordinate $\zeta$ appear as such forms, $\lambda \sin \lambda \zeta$ or $\frac{1}{\lambda} \sin \lambda \zeta$

but, to keep the order of the values of each element uniform, the authors eliminate the linear terms of $\lambda$ as shown in Table 1.

The values of the determinant of the eigen-value equation is smaller than a value of each element of the matrix at the neighbourhood of its roots. So the lowest significant digit of each element must situate at the lower order than that of the determinate in the iteration process. A type of the numerical calculation in the determinant corresponds to

$$\cosh^2 \lambda \xi - \sinh^2 \lambda \xi - 1 = 0 \tag{2.6}$$

in the case of a simple beam. If the lowest significant digit of $\cosh^2 \lambda \xi$ or $\sinh^2 \lambda \xi$ is larger than unity, the value of the equation (6) does not have any meaning for its comparison to zero. The straight line in Fig. 3 is given by the following equation,

$$\log \delta \text{ (number of digits)} = \log \delta_{sc} - 2 \times \lambda \times \log e \tag{2.7}$$

x marks in Fig. 3 also show numbers of significant digits required in the case of $Z$ shaped beam (cf. Fig. 5) for the accuracy $5 \times 10^{-4}$. Two chain lines show the limits, the upper one comes from the word length of the computer (length of double precision word of IBM 7090 is 16 digits) and the lower one comes from the accuracy, which required, of eigen-values $\lambda_j$. In the section beyond the point at which the upper limit crosses the straight line, an approximate root may not situate in the neighbourhood of the real root with the given accuracy $\varepsilon$. Because the approximate root which has been obtained in this section only means two successive values of an approximate root standing within the accuracy $\varepsilon$ by chance on an iteration process.

If we use single precision arithmetic for this computation, in the case of $5 \times 10^{-4}$ accuracy, we would obtained the correct approximate roots only for the section less than $\lambda_j$ is 12.

To obtain the mode shape for each root of the eigen-value or the natural frequency, we have to solve the equation of the supporting condition. The equation in the case of "Fix-Fix" support condition is as follows:

$$\left[ M_{df} \right] \left[ F_0 \right] = \left[ 0 \right] \tag{2.8}$$

Because the determate of $M_{df}$ is equal to zero, we can choose arbitrary one out of the elements in vector $F_0$ and put it as a unit. It is as easily as the whole matrix to obtain the transfer matrix from one end to a point on the beam. The displacement and force at the point $\xi$ are given by the following equation,

$$\begin{bmatrix} D \\ F \end{bmatrix}_\xi = \begin{bmatrix} M_{df} \\ M_f \end{bmatrix}_{0\xi} * \left[ F_0 \right] \tag{2.9}$$

§2.2  Effect of Additional Masses, Dash pots and Springs

There are two ways to take the effect of them into account. One of them is using the transfer matrix expressed as the impedance of the additional element or the branch at the junction point. Of course, for dash pots or other sorts of energy dispersion devices the matrix should be expressed with complex number. The impedance of the branch fixed at the other end can be written as

$$Z = \left[ M_f \right] \left[ M_{df} \right]^{-1} \tag{2.10}$$

$M_f$ and $M_{df}$ are parts of the transfer matrix from the fixed end to the junction.

The other way is as follows: We assume that we already knew the natural frequencies $\nu_j$ and their normal modes $X_j(x)$ of the system, and that we would plan to add some additional elements (masses $m_k$, dash pots $C_k$ and springs $k_k$) to it. The frequency equation is given by the following form.

$$\det. \left| \delta_{\ell k} - \frac{1}{M_t} \sum_j \frac{m_k p^2 - k_k - i C_k p}{\nu_j^2 - p^2} X_j(\ell) X_j(k) \right| = 0$$

$$\ell, k = 1, ---, n \qquad \begin{cases} \delta_{\ell k} = 1 & \text{for } \ell = k \\ \delta_{\ell k} = 0 & \text{for } \ell \neq k \end{cases} \tag{2.11}$$

How the region of $j$ (the number of terms) should be is not definite, but for the minor additional elements only the first term or the first two terms should be considered.

§2.3. Evaluation of the forces and moments under an earthquake loading .

To obtain the moment distribution on the piping, we must calculate the exiting co-efficient $I_j$ and the amplification factor $A$ .( $A = \alpha / \alpha_f$ ref. § 3.) $I_j$ can be calculated from the summation of displacement, of which the direction is parallel to that of the external acceleration, weighting with its mass distribution. $n_j$ represents the factor of normalizing the displacement. Then the displacement and force vector under an external acceleration $f$ becomes.

$$\begin{bmatrix} y \\ \alpha \\ f \\ m \end{bmatrix} = \frac{A I_j f}{n_j} \begin{bmatrix} \frac{1}{\lambda_j^4} \cdot \frac{PL^4}{EI} \times \overline{y} \\ \frac{1}{\lambda_j^3} \cdot \frac{PL^3}{EI} \times \overline{\alpha} \\ PL/\lambda_j \times \overline{f} \\ PL^2/\lambda_j^2 \times \overline{m} \end{bmatrix} \tag{2.12}$$

## 2.4. Examples of the eigen-values and modes

   * Simple beam;  To check the program, the authors choose a simple straight beam.  The eigen-value of the fundamental mode of the fixed beam is calculated as the three pieces one.  It is not necessary to divide a strait section to smaller ones as this example.  Here, the authors only want to check the effects of matrix multiplications.  The interval of steps is 0.1, and the accuracy is changed from $5 \times 10^{-4}$ to $5 \times 10^{-9}$.  (Table 2.) Dr. Young (5) at Texas University got the value in the last row of Table 2, and he guaranteed the accuracy of 8 digits.

   * $Z$ shaped beam;  The second example is $Z$ shaped beam, which consists of three pieces, shown in Fig. 4 and Fig. 5.  The eigen-values of the vibration parallel of the beam to the plane and the perpendicular one are shonw. The values in the lower rows Table 3 are the experimental values obtained with models which are made of steel wire.   The eigen values vs. the length of the third leg are shown in Fig. 4.  This figure may be use for judging the approximate natural frequency of a complex beam.  The examples of mode shape are shown in Fig. 5 and Fig. 6.  The former one is that of the plane $Z$ shaped beam and compared to the deformation curve plotted from the photograph.

   * $L$ shaped beam;  To check the effect of longitudinal vibration, the authors use the in plane vibration of the isosceles $L$ shaped beam.  x marks in Fig. 7 are the values which computed by Professor Takahashi, Yamagata University.

   The authors conclude that the code of this program works properly from the results of the several examples above mentioned.  For these examples, Computer Center of the University of California at Berkeley offered their subsidized time to us.


## 3.  The building-machine structure system response.

   The response spectrum of single-degree-of-freedom linear system is precisely studied by G.W. Housner and his co-workers (6), which simulate the building-structure.  In our country when the atomic power plant construction had been started, the dynamic behaviour of the piping or other machine-structure during earthquake and its aseismic design were newly discussed.  To analyse these problems the analog computer was used, the building, machine-structure system can be simulated two-degree-of-freedom system with appropriate damping coefficient and small mass ratio.  The differential equations are given by (3-1)

$$\begin{cases} \ddot{x}_m + 2\omega_m h_m \dot{x}_m + \omega_m^2 x_m - (2\omega_m h_m \dot{x}_b + \omega_m^2 x_b) = -\alpha(t) \\ -\gamma(2\omega_m h_m \dot{x}_m + \omega_m^2 x_m) + \ddot{x}_b + (2\omega_b h_b + \gamma \cdot 2\omega_m h_m)\dot{x}_b + (\omega_b^2 + \gamma \omega_m^2) = -\alpha(t) \end{cases} \quad (3\text{-}1)$$

when the suffix m, b mean machine and building, that is, upper and lower system respectively, m : mass, $\gamma = m_b/m_m$ : mass ratio, h  : damping ratio to critical damping, $\omega$; no-damped circular frequency, $x$ : relative displacement to the ground of mass Fig. 8 is the response spectrum of upper mass for El Centro earthquake (May 18, 1940) in which the abcissa is the period of the upper system

that corresponds to the machine-structure, the ordinate is the maximum
response of the upper system response.

$\gamma = 0$ means that lower system has no force reaction from upper system.
Points are plotted by the maximum value of responses and the parameter
of several curves is the period of lower mass system. To look over this
results, we need to refer the response spectra of one mass system.
Fig. 9 shows it and it has the extreme value at the period 0.2, 0.5, 0.9 sec.

Now let $T_b$ be the period of lower mass system, $T_m$ that of upper mass
system and $T_g$ the ground dominant period. About the spectrum of $T_b$=0.2 sec
in Fig. 8, the acceleration amplification factor A which is the ratio of
the maximum response to the maximum ground acceleration attains to the
maximum at $T_m$=0.2 sec and for other $T_b$'s it shows also the maximum at
$T_b$=$T_m$ except such example that in case $T_b$=0.8 sec the maximum does not
occur at same $T_m$, but at $T_m$=0.9 sec. These show that the coincidence
of both structure periods should be evaded at first from the viewpoint
of the aseismic design of machine-structure.

Of the velocity and the displacement the fact that when $T_b$=$T_m$, the
response reaches to the maximum for a $T_b$, is not applicable, for example
about the displacement response spectrum in case T is rather small it does
not give the maximum but the extreme at $T_b$=$T_m$ and the maximum occurs at
longer period.

It seems that the period 0.2, 0.5, 0.9 sec have any relation to $T_g$ from
Fig. 9, so its effect to the upper system through the lower system must be
taken into consideration. Thinking of the spectra of $T_b$=0.2, 0.5 sec in Fig.
8. At first about the former, at $T_m$=$T_b$=0.2 sec the amplification factor
reaches to the maximum and the spectrum near $T_m$=0.5 sec does not decrease
steeply but holds rather constant, then it can be supposed that the upper
system receives a little effect of $T_g$. About the latter at $T_m$=0.2 sec it
does not seem to be given the effect of the peak at $T_g$=0.2 sec. To study
these effect, the relation among $T_u$, $T_\ell$ and $T_b$ are examined which will be
mentioned later. Moreover a statistical computation makes it clearer.

About two-mass-spring system in case that the damping of the upper mass
system is very small and $T_b$=$T_m$, the time that the maximum occurs in the
response of a oscillator is further lag than that of earthquake record.
Because the mass is so small that the behaviour shows quasi-resonance and
vibrate nearly with the first mode.

In anyway as for the acceleration, $T_b$=$T_m$ makes the worst condition,
now another spectrum which is shown in Fig. 10 can be driven from Fig. 8 by
connecting such points. The ratio to critical damping is selected as para-
meter. Though the amplification factor is larger than that of one mass
system, figures are analogous to it, let us call it $T_b$-$T_m$ response spectrum
of two-mass-spring system. The same spectra about the velocity and dis-
placement are also analogous, such as the velocity spectrum is constant and
the displacement increases with period.

The effect of damping is remarkable in Fig. 10, this means that in case
the coincidence of both system periods cannot be evaded inevitably, the next
method is to attach the damper between both structures. This can be done be-
cause the machine structure or piping is usually much smaller than the build-

ing-structure.

These analysis are also performed about Kushiro (Dec. 24, 1961), Saitama (Feb. 14, 1956), partly Taft (July 21, 1952) and some results are obtained. for $\gamma=0$, 0.01, $h_b=0.07$

1) When $T_b=T_m$ or $T_b=T_m$, the response of the machine-structure shows the worst condition especially in shorter period about the acceleration, in longer period about the displacement.

2) A at $T_b=T_m$ has the maximum at a period where that of one mass system becomes the maximum.

3) When one mass system response spectrum shows bi-extreme characteristic, in case of two mass system it has the tendency that the maximum occurs at shorter period.

4) The $T_b$-$T_m$ acceleration response spectrum has a maximum for a $T_b$.

5) The $T_b$-$T_m$ velocity and displacement response spectrum show that it is nearly constant and increases for larger period respectively.

6) The tendency that A increases for small or $h_m$ is remarkable near $T_b=T_m$.

7) When $h_m$ is large, the maximum values of $T_b$-$T_m$ response spectra are constant for any earthquake records.

8) If $T_u$, $T_\ell$ are the period where the amplification factor is a half of the maximum for a spectrum of $T_b$, then (for $h_m=0.02$)

$$T_b > T_g : \quad T_u/T_b = 1.2 \quad T_\ell/T_b = 0.6, \quad T_b < T_g : \quad T_u/T_b = 1.6 \quad T_\ell/T_b = 0.7$$

9) If the ground dominant, building-structure, machine-structure periods are know, we can guess the response spectra of two-mass-spring system from $T_b$-$T_m$ response spectra using 8) without computing it precisely.

Such response spectrum computation was also studied in case that only the building structure has the elasto-plastic characteristic. Generally speaking, the amplification factor of machine-structure decreases even when $T_b=T_m$ because the restoring force of lower mass system is limitted. But the period of lower mass spring system is changed apparently, so it makes sometimes the condition worse than that of the linear system considering the number of the repitition during an earthquake. By the analysis of response spectra for El Centro earthquake, the next formula can be induced.

$$A_m' = k \cdot \frac{F_b}{F_g} \cdot \frac{A_m}{A_b} \tag{3-2}$$

where $A_b$ : A of one mass linear response spectrum. $A_m$: A of $T_b$-$T_m$ linear response spectrum. $F_b$: Lower mass acceleration which corresponds to yield force. Fg: Earthquake maximum acceleration. $F_1$: Response acceleration of one mass linear system (which can be given from spectrum) $F_2$: Response acceleration that can be given from linear $T_b$-$T_m$ response spectrum. $F_{N2}$: Upper mass acceleration that can be given from $T_b$-$T_m$ response spectrum of lower mass system nonlinear. $A_m$: Acceleration amplification factor of lower mass system nonlinear $T_b$-$T_m$ response spectrum.

$$k = (F_{N2}/F_2)/(F_b/F_1)$$

$$h_m = 0.007 : \qquad\qquad \hat{k} = 0.8 - 2.0$$
$$h_m = 0.02 \quad : \qquad\qquad \hat{k} = 0.8 - 1.5$$
$$h_m = 0.1, 0.2 : \qquad\qquad \hat{k} = 0.8 - 1.2 \qquad\qquad (3\text{-}3)$$

Thus if we compute linear and nonlinear acceleration repsonse spectrum of one mass system and the linear $T_b$-$T_m$ response spectrum, the rough estimation of $A_m'$ can be done.

4. The statistical computation of response.

To generalise the response computation and to make it easy to know the acceleration amplification factor, a statistical computation (7) was tried. The earthquake was supposed to be a random process which is the stationary time function with gaussian distribution at the basement, has the constant power spectrum, and the ground has the characteristic studied by Kanai (8). Moreover to compute reasonably the high and low pass filter is attached to it, that is,

$$H_g(S) = \frac{2\omega_g h_g S + \omega_g^2}{S^2 + 2\omega_g h_g S + \omega_g^2} \cdot \frac{S^2}{(1+\psi_1 S)^2} \cdot \frac{1}{(1+\psi_2 S)^2} \qquad (4\text{-}1)$$

$\psi_1, \psi_2$ are decided from the breakpoint of the filter characteristic. It is supposed that the maximum will occur when the extreme probability density function $p(y)$ become small enough. $p(y)$ is given as (9) (10)

$$p(y) = \frac{1}{2\pi} \varepsilon \exp\left(-\frac{y^2}{2\varepsilon^2}\right) + y \exp\left(-\frac{y^2}{2}\right)\left(1 + \operatorname{erf}\frac{\sqrt{1-\varepsilon^2}}{\sqrt{2}\varepsilon} y\right) \qquad (4\text{-}2)$$

$$\varepsilon^2 = 1 - \frac{I_2^2}{I_0 I_4} = 1 - \left(\frac{N_e}{N_0}\right)^2, \qquad y = \frac{I}{\sqrt{I_0}} \qquad (4\text{-}3)$$

$$I_0 = \frac{1}{2\pi}\int_0^\infty h(\omega)d\omega \qquad I_2 = \frac{1}{2\pi}\cdot\frac{1}{4\pi^2}\int_0^\infty \omega^2 h(\omega)d\omega \qquad I_4 = \frac{1}{2\pi}\cdot\frac{1}{16\pi^4}\int_0^\infty \omega^4 h(\omega)d\omega \qquad (4\text{-}4)$$

where $I$ : the amplitude $N_0$ : the number of zero with positive slope
$N_e$: the number of extreme
As for the machine structure $h(\omega)$ is,

$$h(\omega) = \left|\frac{(2\omega_m h_m S + \omega_m^2)(2\omega_b h_b S + \omega_b^2)}{\Delta} H_g(S)\right|^2 \qquad (4\text{-}5)$$

$$\Delta = S^4 + \{2\omega_b h_b S + (\gamma+1)\,2\omega_m h_m\} S^3$$
$$+ \{\omega_b^2 + (\gamma+1)\omega_m^2 + 2\omega_b h_b \cdot 2\omega_m h_m\} S^2$$
$$+ \{\omega_b^2 \cdot 2\omega_m h_m + \omega_m^2 \cdot 2\omega_b h_b\} S + \omega_b^2 \cdot \omega_m^2$$

The integration is performed by the formula shown in (11)
Fig. 11 is an example of the extreme distribution of an earthquake record. $\varepsilon$ can be given by the number of zero and extreme, for the same $\varepsilon$ (4-2) also can be computed. Comparing with both curves, maximum of both distribution were coincided with. After then where $p(y) = 0.01$

and $\overset{y}{\smile}$ where the distribution about earthquake record is equal to zero are refered. The result is shown in Fig. 11 (b). It shows that $y$ of $p(y)=$ 0.01 is quite a good measure appropriate as the representation of the maximum. For the random process that corresponds to the earthquake and the response for it, $y$'s are computed as $y_m$, $y_j$ respectively and the response amplification factor is given

$$A_m = \frac{\alpha_m}{\alpha_j} = \frac{\sqrt{I_{om}}}{\sqrt{I_{oj}}} \cdot \frac{y_m}{y_j} \qquad (4\text{-}6)$$

The response spectrum and the statistical computation above mentioned are compared with in Fig. 12, (a) is as for one mass spring system, (b) is as for two mass spring system. In any case the statistical computation covers the response spectrum as an evelope. But about the latter when the $h_m$ is very small, the amplification of response spectrum is smaller than that of the statistical analysis. It seems to be so because of the discrepancy which the real earthquake is not stationary though the supposition of statistical computation is stationary.

Taking into these supposition, the table by the statistical computation for the various parameter will be useful for the estimation of the machine-structure response acceleration. The effect of the ground period characteristic to the machine-structure through the building-structure is also clarified. By Fig. 13 if $T_b > T_g$ , the effect is hardly seen, and when $T_b < T_g$, the spectrum has two peaks, that is where $T_m = T_b$ and $T_m = T_g$. But at any rate it shows the maximum when $T_m = T_b$.

In Fig. 12 the spectrum of a model earthquake is also shown. It realises the statistical computation experimentally using the analog computer and a noise generater.

Such statistical computation can be extended to a nonlinear system with elasto-plastic characteristic. The system model is shown in Fig. 14. The equation is,

$$\begin{cases} m\ddot{x} = -u\dot{x} - f - m\alpha(t) \\ f = ky \\ \dot{x} = \dot{y} & \qquad f < |F| \\ f = F \frac{\dot{x} - \dot{y}}{|\dot{x} - \dot{y}|} & \qquad f \leqslant |F| \end{cases} \qquad (4\text{-}7)$$

where m : mass, $u$: damping coefficient, $k$ : spring constant
    $x$ : relative displacement to the ground of the mass
    $y$ : relative displacement to the ground of the upper part of spring
    $F$ : yield force
    $\alpha(t)$: earthquake acceleration

The block diagram of the system is also shown in Fig. 14. If $Z = \dot{x} - \dot{y}$ and for nonlinear element the equilinearized method (12) is used, the next equation can be written.

$$\chi = \sqrt{\frac{Z}{\pi}} \frac{H}{\sqrt{I_z}} = \sqrt{\frac{Z}{\pi}} \frac{\alpha\sqrt{I_g}}{\sqrt{I_z}} \tag{4-8}$$

$$I_z = \frac{1}{2\pi}\int_0^\infty |Z(s)|^2 d\omega \tag{4-9}$$

$$Z(s) = \frac{\omega_b^2}{\chi s^2 + (\omega_b^2 + 2\omega_b h_b \chi)s + \omega_b^2(2\omega_b h_b + \chi)} H_g(s) \tag{4-10}$$

$\chi$ is equi-linear gain of nonlinear element by the criterion so as to minimise the integration of square error by the substitution. Solving (4-8) and (4-9), $I_\chi$ is given. The $I_x$ is calculated using $\chi$

$$I_x = \frac{1}{2\pi}\int_0^\infty |\chi(s)|^2 d\omega \tag{4-11}$$

where

$$\chi(s) = \frac{1}{s}(1 + \frac{\chi}{\omega_b^2}s)Z(s) \tag{4-12}$$

$\sqrt{I_x}$ is proportional to the displacement response, so it is necessary to make the value nearly equal to the displacement properly. Fig. 15 shows an example as $T_g = 0.5$ sec, some characteristics can be seen in it.

1) The displacement spectra becomes larger in longer period.
2) If $\alpha$ becomes small, which means the yield force becomes small and the nonlinearity strong, the displacement of the nonlinear system is larger than that of linear one in short period.
3) At the same time the cross point of both response spectra moves to longer period.
4) If $\alpha$ becomes large, the figure of the nonlinear system comes near to that of the linear system, in short period from larger side, in longer period from smaller one, the cross point transfer to shorter period.

These are also found in the results (13) (14) that have been studied by the response computation.

Using Fig. 15 the optimum seismicity (15) also can be explained and from (4-12) the spectrum of velocity vs. the period can be obtained.


5. Acknowledgement

Reference

1. Takeyama, K. and his committee, "Reactor Safety and Hazards Evaluation Techniques", Proc. of I.A.E.A. Conferense at Vienna, p. 179, May 1962.

2. Shibata, H. and Shigeta, T., "On a Dynamic Behavior of a Piping System", Proc. of Japan National Symposium on Earthquake Engineering, p. 183, Nov. 1962.

3. Shibata, H. and Shigeta, T. "On a Dynamic Behavior of a Piping System", Trans. of the Japan Society of Mechanical Engineers, Vol. 29, No. 200, April 1963.

4. Okumura, A. "On a Method of Analysis for Vibration and Stability Problems of Linear Mechanical Systems or Structures", Mem. Fac. of Sci. and Eng., Waseda University, No. 21, 1957.

5. Young, D. and Felgar, R.P., University of Texas Publishing, No. 4913, 1949.

6. G.W. Housner, R.R Martel and J.L. Alford, "Spectrum Analysis of Strong Motion Earthquakes" Bull. Seism. Soc. Am., Vol. 43, No.2, April 1953.

7. H. Tajimi, "Basic Theory on Aseismic Design of Structures" Rep. The Inst. of Industrial Science, Univ. of Tokyo Vol. 8, No.4, March 1959.

8. K. Kanai, "Semi-experiment Formula on the Dynamic Characteristic of Ground" Rep. of AIJ No. 57. 1967.

9. S.O. Rice, "Mathematical Theory of Random Noise" BSTJ, 1944 - 1945.

10. D.E. Cartright and M.S. Longuet-Higgins," The Statistical Distribution of the Maxima of a Random Function" Proc. of the Royal Soc. of London No.237, 1956.

11. H.M. James, N.B. Nichols and R.S. Philips, "Theory of Servomechanisms" MIT R.L. Series vol. 25, McGraw Hill. N.Y., 1947.

12. Y. Sawaragi, "A Survey on the Statistical Study for Nonlinear Control Systems", Rep. The Inst. of Tech. Univ. of Kyoto No.14, 1958.

13. G.V. Berg and S.S. Thomadies, "Effect of Inclastic Action on the Behaviour of Structures During Earthquakes" IIWCEE 1960.

14. H. Sato, "Study on Aseismic Design of Machine Structures", The paper of doctorate Faculty of Engg. Univ. of Tokyo 1963.

15. Y. Osawa and A. Shibata, "A Characteristic of Nonlinear Response for Earthquake" Rep. of AIJ No.69, 1961.

$$
\begin{array}{c|cccccccccccc}
 & x & y & z & \alpha & \beta & \gamma & f_x & f_y & f_z & M_\alpha & M_\beta & M_r \\
\hline
x & c+ch & 0 & 0 & 0 & s+sh & 0 & -s+sh & 0 & 0 & 0 & -(c+ch) & 0 \\
y & 0 & c+ch & 0 & s+sh & 0 & 0 & 0 & -s+sh & 0 & -c+ch & 0 & 0 \\
z & 0 & 0 & C_1 & 0 & 0 & 0 & 0 & 0 & -r\lambda S_1 & 0 & 0 & 0 \\
\alpha & 0 & -s+sh & 0 & c-ch & 0 & 0 & 0 & -(c-ch) & 0 & s-sh & 0 & 0 \\
\beta & -s+sh & 0 & 0 & 0 & c+ch & 0 & -c+ch & 0 & 0 & 0 & -(s\,sh) & 0 \\
\gamma & 0 & 0 & 0 & 0 & 0 & C_2 & 0 & 0 & 0 & 0 & 0 & -\sqrt{\tfrac{1+v}{2}}\tfrac{1}{r}\lambda S_2 \\
f_x & s+sh & 0 & 0 & 0 & -c+ch & 0 & c+ch & 0 & 0 & 0 & -(s+sh) & 0 \\
f_y & 0 & s+sh & 0 & c\,ch & 0 & 0 & 0 & c+ch & 0 & -s+sh & 0 & 0 \\
f_z & 0 & 0 & r\lambda S_1 & 0 & 0 & 0 & 0 & 0 & C_1 & 0 & 0 & 0 \\
M_\alpha & 0 & -c+ch & 0 & -(s+sh) & 0 & 0 & 0 & s+sh & 0 & c+ch & 0 & 0 \\
M_\beta & -(c+ch) & 0 & 0 & 0 & -(s+sh) & 0 & s+sh & 0 & 0 & 0 & c+ch & 0 \\
M_r & 0 & 0 & 0 & 0 & 0 & \sqrt{\tfrac{2}{v+1}}\,r\lambda S_2 & 0 & 0 & 0 & 0 & 0 & C_2
\end{array}
$$

$$c = \tfrac{1}{2}\cos\lambda\xi \qquad C_1 = \cos r\lambda^2\xi$$

$$s = \tfrac{1}{2}\sin\lambda\xi \qquad S_1 = \sin r\lambda^2\xi$$

$$ch = \tfrac{1}{2}\cosh\lambda\xi \qquad C_2 = \cos\sqrt{2(1+v)}\,r\lambda^2\xi$$

$$sh = \tfrac{1}{2}\sinh\lambda\xi \qquad S_2 = \sin\sqrt{2(1+v)}\,r\lambda^2\xi$$

TABLE 1   TRANSFER MATRIX OF ELEMENTARY BEAM

| RELATIVE ACCURACY | $\lambda_1$ | RESIDUE OF DET. |
|---|---|---|
| $5 \times 10^{-4}$ | 4.729847 | $3.4 \times 10^{-2}$ |
| $5 \times 10^{-7}$ | 4.7300406 | $1.7 \times 10^{-5}$ |
| $5 \times 10^{-9}$ | 4.7300407 | $1.1 \times 10^{-7}$ |
| UNIV. OF TEXAS | 4.7300408 | ———— |

TABLE 2   COMPARISON OF EIGE VALUE OF SIMPLE BEAM

VIBRATION PARALLEL TO PLANE OF BEAM

| THEORETICAL | 6.8385 | 8.7318 | 12.0925 | 15.4027 | 20.0659 | 22.0947 |
|---|---|---|---|---|---|---|
| EXPERIMENTAL | 6.77 | 8.69 | 12.02 | 15.5 | —— | —— |

VIBRATION PERPENDICULAR TO PLANE OF BEAM

| THEORETICAL | 4.2859 | 8.2131 | 8.9667 | 13.0626 | 15.5077 | 20.3779 | 22.2851 |
|---|---|---|---|---|---|---|---|
| EXPERIMENTAL | 4.28 | 8.17 | 8.96 | —— | —— | —— | —— |

TABLE 3   EIGN VALUES OF Z-SHAPED BEAM IN PLANE

SPRING

k

MASS

③

②

[M₂]

①

[M₁]

$L_1$

z

x y

x y

z

z

x y

φ

φ

0

1

2
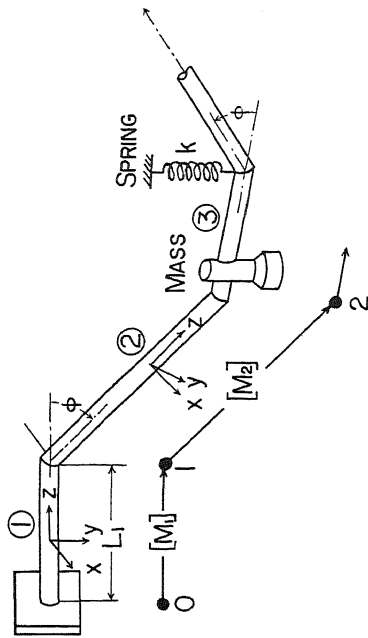
FIG. 2 SCHEMA AND NOMENCLATURES OF COMPLEX SHAPED BEAM

NUMBER OF ORDER
REQUIRED FOR 3 DIGIT ACCURACY OF RESULT

25

20

15

10

5

3

LIMIT BY CAPACITY
OF COMPUTER

LIMIT OF REQUIRED
ACCURACY

6   10   15   20   25   30   35

LAMBDA
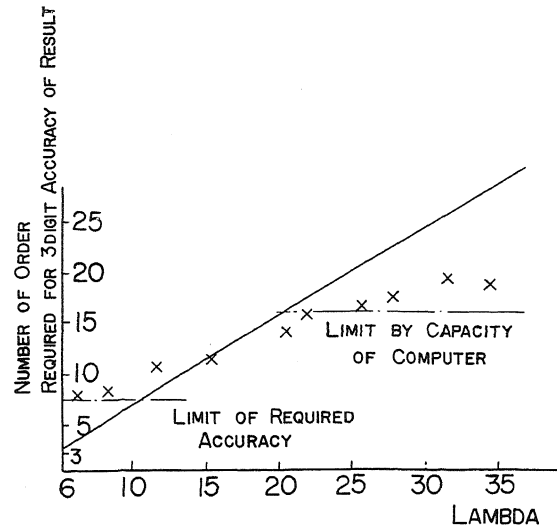
FIG. 3   LIMIT OF ACCURACY AND NUMBER
OF DIGIT REQUIRED FOR
COMPUTATION OF EIGEN VALUE

EVALUATION OF
NATURAL
FREQUENCY AND
MODE SHAPE

COMPUTATION OF
RESPONSE OF
THE SYSTEM
ON EACH MODE

SUMMING UP
THE EACH
RESPONSE TO
THE RESPONSE
OF WHOLE
SYSTEM

CHECK OF THE
RESPONSE
AGAINST THE
DESIGN
CRITERIA

ANALYSIS OF
THE STRONG
EARTHQUAKE
MOTION

SYNTHESIS OF
PSEUDO
EARTHQUAKE
MOTION
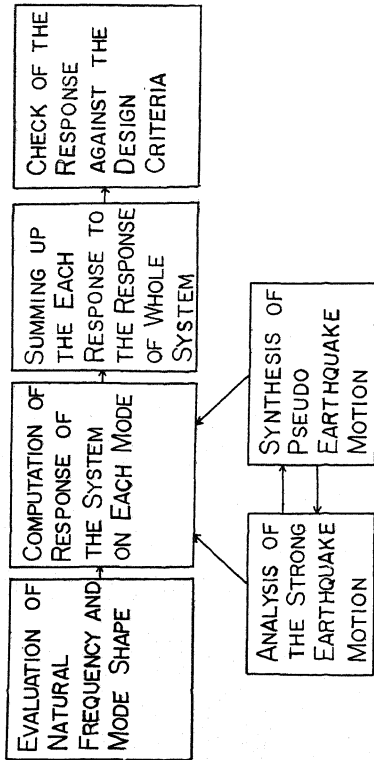
FIG. I   SCHEMATIC FLOW CHART OF ASEISMIC DESIGN

EIGEN VALUE $\lambda$

14

12

10

8

6

4

3

2

3

X, ● EXPERIMENTAL VALUES
△ CALCULATED VALUES
◑ CALCULATED VALUES OF
PLAN BEAM

0   1   2   3   4   5   6

$L_3$   LENGTH OF THE THIRD LEG
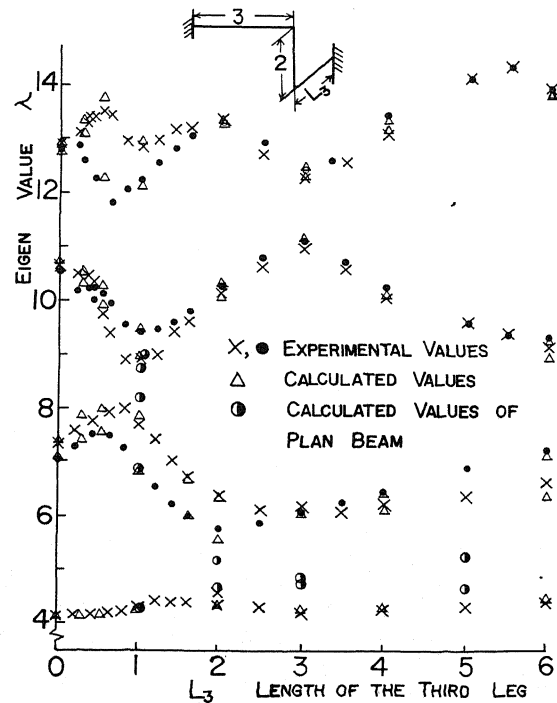
FIG. 4   EIGEN VALUE OF THREE DIMENSIONAL
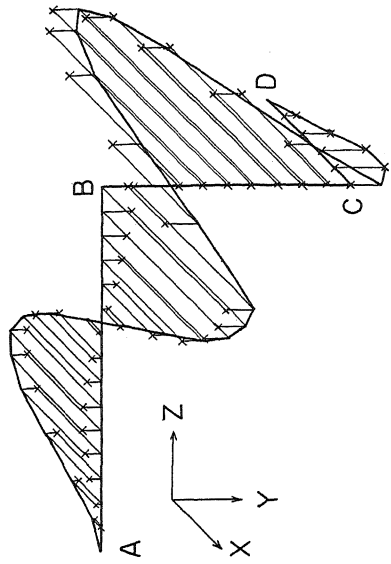Z SHAPED BEAM VS. LENGTH OF
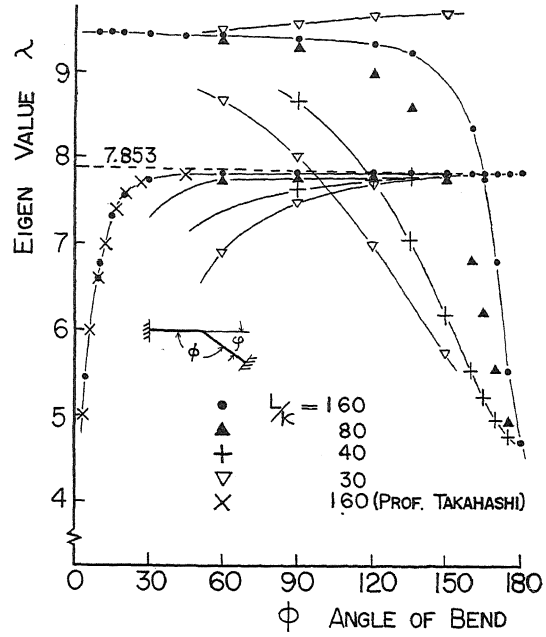THE THIRD LEG

FIG. 6  A MODE OF THREE DIMENSIONAL
Z-SHAPED BEAM



FIG. 7  EIGEN VALUE OF L SHAPED BEAM
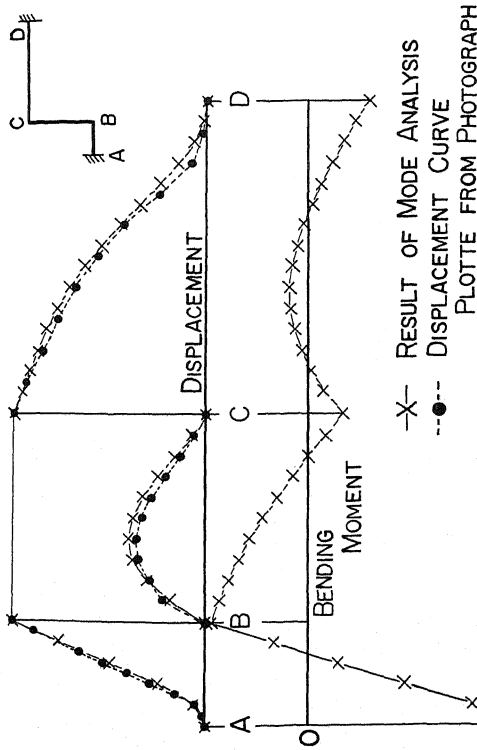VS. ANGLE OF BEND



FIG. 5  A MODE OF Z SHAPED BEAM IN PLANE

—X— RESULT OF MODE ANALYSIS
---●--- DISPLACEMENT CURVE
PLOTTE FROM PHOTOGRAPH



FIG. 8 THE RESPONSE SPECTRUM
OF TWO-MASS-SRRING SYSTEM

| Tb SEC | | γ = 0 |
| --- | --- | --- |
| 0.2 | | hb = 0.07 |
| 0.3 | | hm = 0.02 |
| 0.4 | | |
| 0.5 | | |
| 0.6 | | |
| 0.8 | | |
| 1.0 | | |

Fig.9 The Response Specrum of One-Mass Spring System
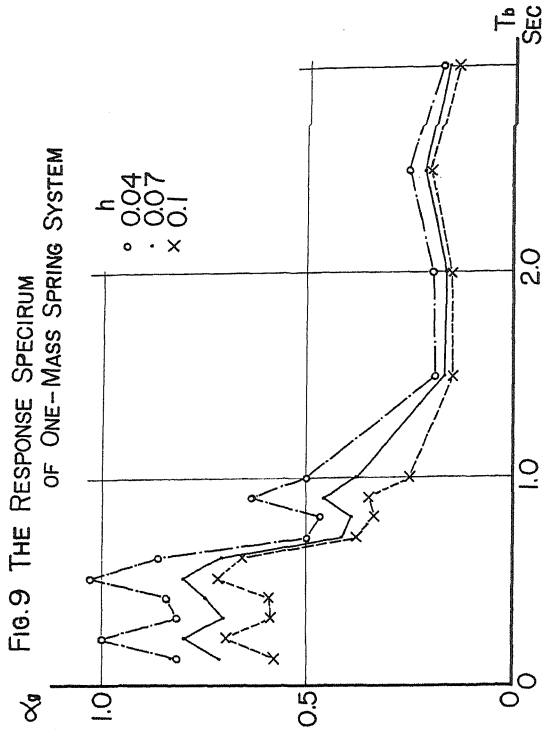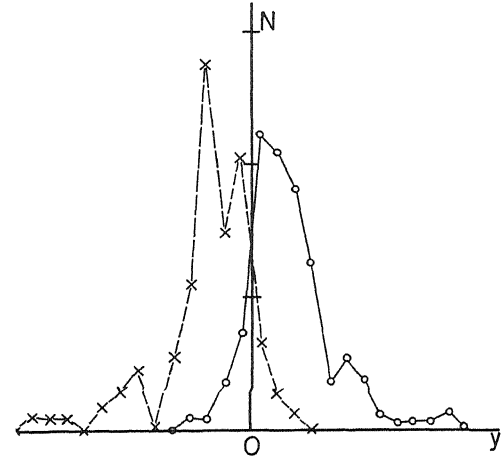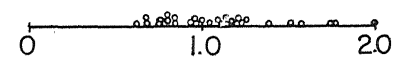


Fig.10 $T_b - T_m$ Response Spectrum
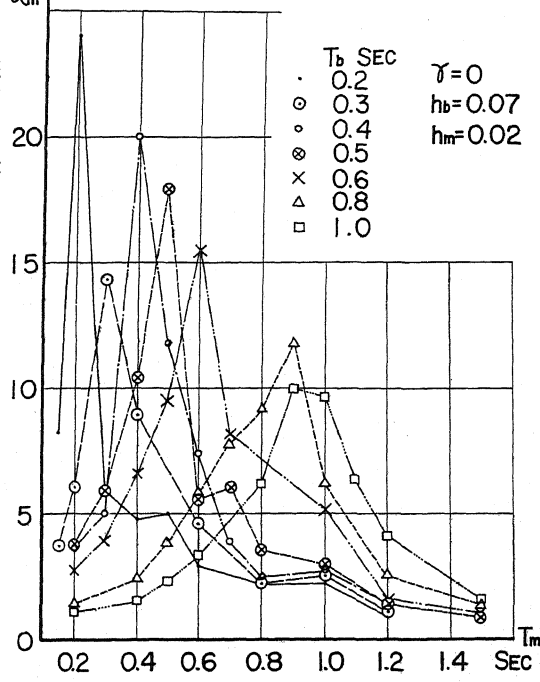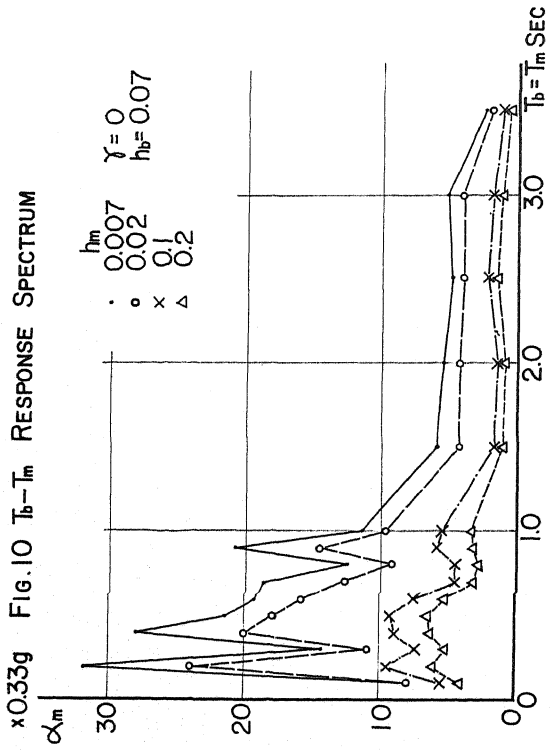


Fig.11 (a) An Example of the Extreme Density Distribution of an Earthquake

(b) Comparison with the Maximum and Y Where p(y)=0.01

FIG.12 THE RESPONSE SPECTRUM AND THE STATISTICAL COMPUTATION
(b) ONE MASS SYSTEM

△ELCENTRO
○ KUSHIRO
⊗ TAFT
× SAITAMA
□ MODEL EARTHQ

$h_b=0.07$
$h_g=0.4$
$h_g=0.5$

$\alpha_b/\alpha_g$

$T_b/T_g$



FIG.12 THE RESPONSE SPECTRUM AND THE STATISTICAL COMPUTAION
(a) TWO MASS SYSTEM

・ELCENTRO
○ SAITAMA
△ KUSHIRO
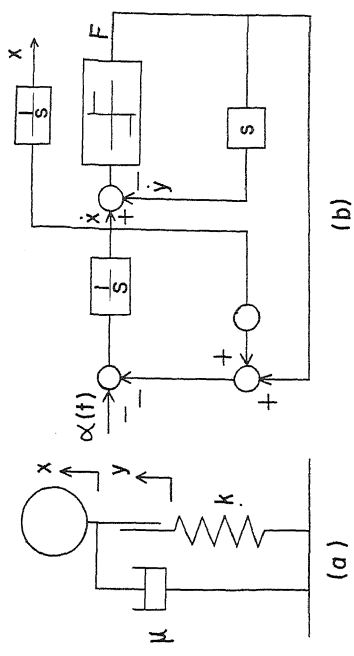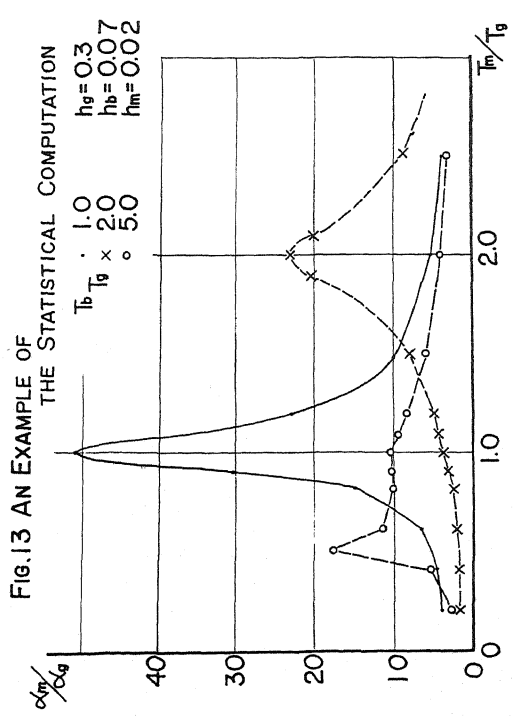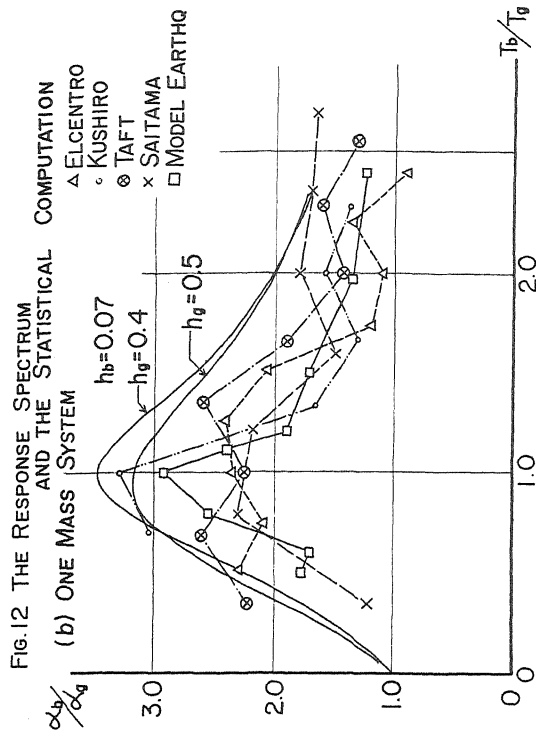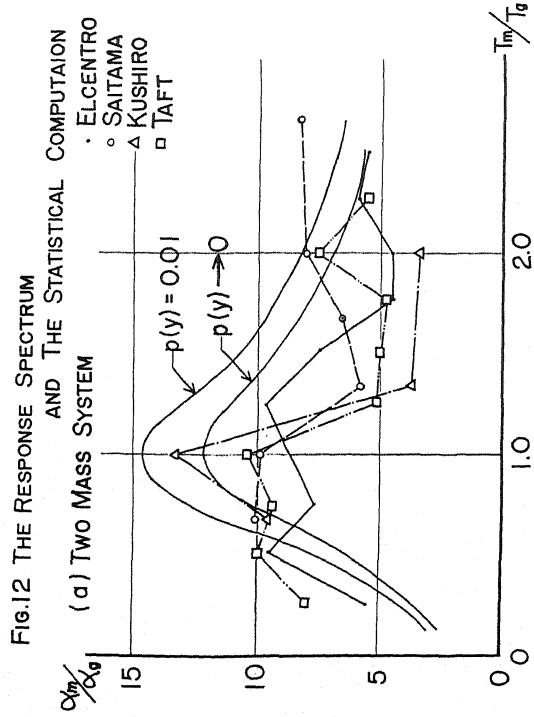□ TAFT

$p(y)=0.01$
$p(y)\longrightarrow O$

$\alpha_m/\alpha_g$

$T_m/T_g$



FIG.14 A MODE OF NON LINER OSCILLATER AND THE BLOCK DIAGRAM

$\alpha(t)$

$F$

$\dot{x}$

$\dot{y}$

$x$

$k$

$\mu$

(a)

(b)



FIG.13 AN EXAMPLE OF THE STATISTICAL COMPUTATION

$h_g=0.3$
$h_b=0.07$
$h_m=0.02$

$\dfrac{T_b}{T_g}$ ・ 1.0
× 2.0
○ 5.0

$\alpha_m/\alpha_g$

$T_m/T_g$

II—567

# FIG.15 THE STATISTICAL COMPUTATION
##                    FOR NONLINEAR SYSTEM



(a) DISPLACEMENT

$\sqrt{I_x}$

$\alpha$

⊙   1/10
∘   1/3
×   2/3
□   1
△   1.5
·   $\ell$
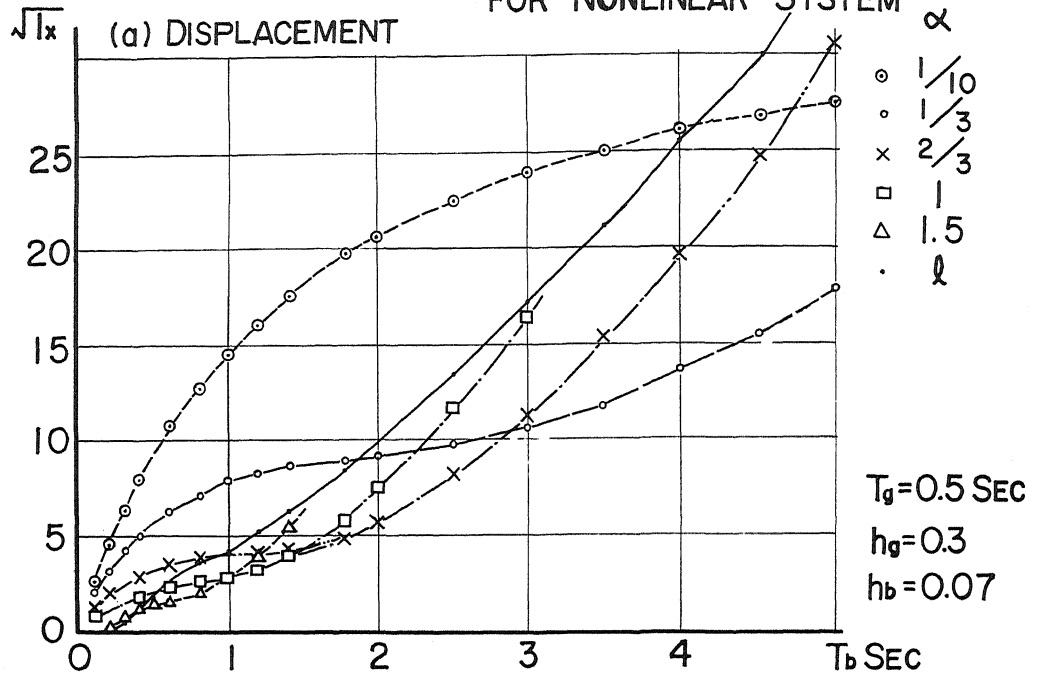
$T_g = 0.5$ SEC
$h_g = 0.3$
$h_b = 0.07$

$T_b$ SEC

# FIG.15 THE STATISTICAL COMPUTATION
##                    FOR NONLINEAR SYSTEM



(b) VELOCITY

$\sqrt{I_v}$

$\alpha$

×   2/3
□   1
△   1.5
∘   1/3
·   $\ell$

$T_g = 0.5$ SEC
$h_g = 0.3$
$h_b = 0.1$

$T_b$ SEC